Quasi-one-dimensional excitons in lateral surface-induced superlattices

G. H. Cocoletzi
Instituto de Física Universidad Autónoma de Puebla, Apartado Postal J-48, Puebla 72570, Mexico

S. E. Ulloa
Department of Physics and Astronomy and Condensed Matter and Surface Sciences Program, Ohio University, Athens, Ohio 45701-2979

(Received 6 December 1999; revised manuscript received 17 February 2000)

We study the effects of an electrostatic potential designed to induce a lateral periodic modulation in a quantum well. The resulting superlattice, for small periods, is a system where quasi-one-dimensional excitons can tunnel from one effective potential well to the next and exhibit a unique center-of-mass folded dispersion which should be accessible to photoluminescence experiments. An effective-mass envelope-function approach is used to estimate resulting excitonic minibands, binding energies, and absorption coefficients for the ground and first few excited states of heavy-hole excitons. For strong electrostatic confinement, this configuration strongly polarizes the excitons, resembling a type-II superlattice where electrons and holes are spatially separated in different potential wells. A competition between quantum structural confinement and Coulomb interactions is evident in the exciton features.

Optical and electronic properties of semiconductor heterostructures and superlattices have been one of the most active research areas in recent years.[1] Special interest has been paid to excitonic transitions in single, coupled pairs, and multiple quantum wells, both theoretically and experimentally. Quantum confinement as well as the effects of applied electric and magnetic fields have demonstrated to significantly affect the binding energies and the absorption coefficients of excitons in these systems.[1] On the other hand, recent experimental studies of the optical properties of quantum wells with a *lateral* field-effect-induced superlattice potential have shown that the photoluminescence (PL) and excitation (PLE) spectra exhibit a strong dependence on applied voltages.[2] The basic design involves depositing a series of parallel metallic lines on a plane close to a quantum well or heterojunction [see the inset in Fig. 1(b)]. Further investigations on these systems have explored potential applications in electro-optic devices.[3,4] These experiments show that through clever sample design and voltage controls, it is possible to spatially separate optically produced carriers and then purposely allow their recombination at desired positions and times.

In this paper, we propose a natural extension of such system: One where the separation between gate voltage ''fingers'' is short enough to allow carrier tunneling from one quasi-one-dimensional potential well to the next. This regime, which is at the edge of technical feasibility at present time (as it requires periods of a few hundred angstrom), would allow the fabrication of an excitonic superlattice with controllable features and unique multiple PL and PLE features at low temperatures. We believe that these systems will become available in a short time and study their properties.

The proposed structure is similar to the excitonic superlattices that have been proposed and observed in multiple quantum wells.[5] There, however, as in other compositional superlattice potential modulations, it is not possible to change the structural features in a given sample. Moreover, the exciton dispersion that results when the barriers are low and thin enough to allow tunneling still reflects the two dimensionality of the quantum wells, and the optical response is not affected significantly. The additional reduction in dimensionality allowed in the lateral superlattices of Refs. 3 and 4, with short periods, produces a strong modulation of the dispersion relation of the exciton, inducing a ''band fold-

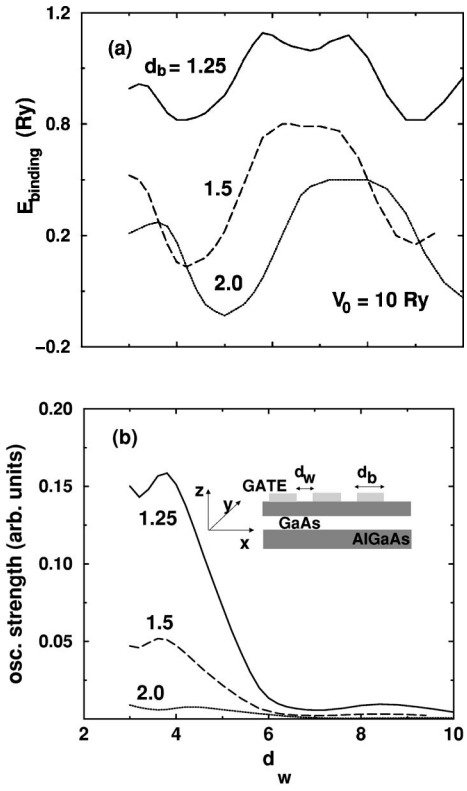

FIG. 1. (a) Exciton binding energies (in Ry, here 5.2 meV) vs d_w for different parameter values. $d_b(d_w)$ is the barrier (well) width for electrons in structure (reversed role for holes), expressed in units of $a_0 = 110$ Å. (b) Oscillator strength for same states. Inset: diagram of structure; both electrons and holes reside in GaAs z well but are laterally modulated by top gate fingers.

ing'' of the dispersion of the center of mass, yielding possible new features in PLE experiments, as we show below.

Although this design could be implemented in a variety of structures, we consider here the case where the finger-gate structure is deposited close to an $Al_xGa_{1-x}As$-GaAs-$Al_xGa_{1-x}As$ quantum well. The quantum well confines carriers in the z direction, and after the application of a strong bias voltage, the finger gate induces an x-direction lateral superlattice modulation (while carriers are still free to move in the y direction). In the limit of strong electrostatic confinement, the situation studied here resembles the excitons in type-II superlattices,[6] where the electron and hole are confined in spatially separated one-dimensional wells, with widths d_w and d_b, respectively, for positive gate voltages.

We explore the effects of this induced lateral confinement on the optical properties via an effective-mass description of the electron and hole Hamiltonian. Using a variational approach similar to that of Dignam and Sipe[5] and others,[7,8] we write the wave function of the exciton as the product of a function depending on the relative coordinates, and the single-particle wave functions of the individual electron and hole appropriate for the geometry of interest. The resulting generalized eigenvalue problem is then solved for the first few states in a tight-binding (weak interwell coupling) limit, where the first experimental structures in that regime are likely to be.

Neglecting possible band nonparabolicities, the Hamiltonian of the excitons in the system under study can be written as

$$H = T - \frac{e^2}{\varepsilon|\mathbf{r}_e - \mathbf{r}_h|} + U_z(z_e, z_h) + U_x(x_e, x_h), \tag{1}$$

where T is the kinetic-energy operator for both the electron and hole, ε is the static dielectric constant, $\mathbf{r}_e$ and $\mathbf{r}_h$ are the electron and hole coordinates, $U_z(z_e, z_h) = U_e(z_e) + U_h(z_h)$ describes the structural confinement provided by the quantum well, and

$$U_x(x_e, x_h) = \sum_m \left[V_e(x_e - md) + V_h(x_h - s_m) \right] \tag{2}$$

is the electrostatic confinement, with m an integer, $s_m = (m + 1/2)d$, and a square profile is assumed,[9]

$$V_j(x_j) = \begin{cases} V_0, & |x_j| \leq d_j/2 \\ 0, & \text{otherwise} \end{cases} \tag{3}$$

for $j = e$ or h. Notice that the source of the modulation is electrostatic and only the charge sign is different for both carriers, so that $V_h(x_h) = -V_e(x_e \to x_h)$, which makes the electron barrier the hole well and vice versa.

The solution of the Schrödinger equation may be written as $\Psi(\mathbf{r}_e, \mathbf{r}_h) = e^{iK_y Y}\Phi(\mathbf{r}_e, \mathbf{r}_h)$, where Y and K_y are the coordinate and momentum of the exciton center of mass along the unmodulated y direction, and Φ represents the solution that accounts for all the confinement. Notice that as the periodic modulation is along the x direction, the center-of-mass momentum along that axis is no longer a good quantum number, and the states can only be written as a Bloch function in X, $\chi^q(x, X) = e^{iqX}u^q(x, X)$, where $X = (m_e x_e + m_h x_h)/M$, $x = x_e - x_h$, $|q| \leq \pi/d$, and $u^q(x, X)$ is a periodic function in X with period $d = d_b + d_w$. Following Ref. 5, we expand the Bloch functions in terms of the corresponding Wannier basis functions centered at each mth period, $W_n(z_e, z_h, y, x, X - md)$, as they provide a convenient representation for the solution of the problem, especially in the limit of weak tunneling between the *lateral* potential wells.

One should emphasize that this description of ''laterally indirect'' excitons is valid only for short periods of the lateral modulation, since for longer periods (much larger than the exciton radius/size), the excitons would drift towards the regions of low field *gradient* and lie on the same spatial region (such as demonstrated in the experiments of Ref. 4), if they survive recombination or ionization. Because realizable devices will be in this ''marginal tunneling'' regime, we consider the periodic modulation as a weak perturbation to the *local* solutions. This ''tight-binding'' limit, where one uses local-well orbitals ϕ^m centered on the well m, provides a convenient approach. Correspondingly, one arrives at the generalized eigenvalue equation,

$$H_{ij}^q b_j^n = E_n A_{ij}^q b_j^n \tag{4}$$

where $H_{ij}^q = \langle \chi_i^q | H | \chi_j^q \rangle$, $A_{ij}^q = \langle \chi_i^q | \chi_j^q \rangle$, and

$$|\chi_j^q\rangle = \frac{1}{\sqrt{N}} \sum_m e^{iqmd} |\phi_j^m\rangle,$$

$$H_{ij}^q = \epsilon_j A_{ij}^q + \sum_m e^{-iqmd} \langle \phi_i^m | \Delta U_j^0 | \phi_j^0 \rangle, \tag{5}$$

where ϵ_j is the isolated-well eigenvalue, $H_j^m |\phi_j^m\rangle = \epsilon_j |\phi_j^m\rangle$. The perturbation potential is given by the difference between the total (periodic) potential and the local-well term (just as in the usual tight-binding description). The generalized eigenvalue problem is solved conveniently in this tight-binding approach, suitable for large electrostatic modulation V_0 [see Eq. (3)].

The analytical solution of the alternate-well electron-and-hole problem with the additional attractive interaction is not possible. The algebraic complications for even the noninteracting case (where the single-particle problem gives rise to transcendental eigenvalue equations, for example), make obtaining the full solution of this reduced problem quite difficult. As in related problems, we adopt a variational solution, which includes the physics of the lateral confinement for each particle, in addition to the correlation introduced by the Coulomb interaction. For each particle in a well, we use

$$\Psi_i(\mathbf{r}_e, \mathbf{r}_h) = \frac{c_0}{\lambda} e^{-r/\lambda} \psi_{il}(\mathbf{r}_e, \mathbf{r}_h), \tag{6}$$

with $\psi_{il}(\mathbf{r}_e, \mathbf{r}_h) = \psi(\boldsymbol{\rho}_e, \boldsymbol{\rho}_h) f_i^e(x_e) f_l^h(x_h - s_1)$, and $\mathbf{r}_j = (x_j, \boldsymbol{\rho}_j)$, $j = e, h$, and $r = |\mathbf{r}_e - \mathbf{r}_h|$. In this equation, f_i^e and f_l^h are the wave functions of the electron and hole for the isolated wells, respectively. The expressions we use are (when each well is centered at the origin)

$$f_l^j = \begin{cases} A e^{\alpha x_j}, & x_j \leq -d_j/2 \\ B \cos(k^j x_j + \delta_l), & |x_j| \leq d_j/2 \\ C e^{-\tau x_j}, & x_j \geq d_j/2, \end{cases} \tag{7}$$

where δ_l is a parameter that vanishes for the ground state and is chosen as $-\pi/2$ for the first excited state, d_j is the potential well width, $k^j=\sqrt{2m_jE_j}/\hbar$ is the wave number in the isolated well, and

$$\psi(\rho_e,\rho_h)=D\cos(q_{ze}z_e)\cos(q_{zh}z_h)e^{iK_yY}. \tag{8}$$

Notice that λ is the *only* free variational parameter, as k^j is determined from the solution of the *finite-height* quantum well in the x direction (allowing for barrier penetration), and $q_z=\pi/a_z$ is the wave vector in the z direction, with well thickness a_z. The constants c_0, α and τ, as well as A to D are calculated using the boundary and normalization conditions of the wave function for the single-well problem.

After calculation of these local two-particle states, $\phi_{jl}^m=f_j^e(x_e-md)f_l^h(x_h-s_m)$, we proceed to calculate the lateral superlattice states $E_n(q)$, as in Eq. (4), for each combination of electron and hole states. Since we are in a situation where electrons and holes can tunnel from well to well, the two-well states have bonding and/or antibonding character, and can be defined with definite parity. The lowest four superlattice bands can then be labeled by $E_1^{\pm}(q)$ and $E_2^{\pm}(q)$, where each band is made from symmetric $(+)$ and antisymmetric $(-)$ combinations of particles in neighboring wells. Notice that the ''1'' states are formed from $\delta=0$ in Eq. (7), while the ''2'' states have $\delta=-\pi/2$. The tight-binding approximation used produces effectively a $\cos(qd)$ dispersion relation, with characteristic bandwidths for each band, as will be shown below.

In all figures below we have used GaAs parameters, with electron mass $m_e=0.067m_0$, heavy-hole mass $m_h^H=0.377m_0$, where m_0 is the bare mass, $\varepsilon=12.2$, and $a_z=50$ Å. These values yield an effective exciton Rydberg, $\mathrm{Ry}=\mu e^4/2\hbar^2\varepsilon^2=5.2$ meV, with the reduced mass $\mu^{-1}=m_e^{-1}+m_h^{H-1}=1/0.057m_0$, and an effective exciton Bohr radius $a_0=\varepsilon\hbar^2/\mu e^2=110$ Å. We measure all relevant quantities in terms of these natural scales.

To help our understanding of the physics in the problem, we calculate the binding energy of the exciton, defined as $E_{binding}=E_0-E_n(q=0)$, where E_0 is the ground-state energy of the uncorrelated electron-hole pair, i.e., the solution to the problem of the two particles in the absence of Coulomb interaction. As the structural parameters will play an important role in controlling the competition between the potential confinement and the attractive interaction between the carriers, one would expect $E_{binding}$ and other features to be strongly affected. Figure 1(a) shows $E_{binding}$ for one of the lowest exciton bands, E_1^+, for different potential parameters.

Notice that for $V_0=10$ Ry, and various values of the electron (hole) barrier (well) d_b, one sees oscillations in $E_{binding}$, arising from a competition between confinement and Coulomb interaction, as seen in Ref. 10 for a similar single-well case. Clearly too, larger d_b yields less binding, as it reduces particle interwell tunneling and effective electron-hole overlap. Notice that for some values of d_w, for the larger d_b, negative binding energies arise from the much reduced electron-hole overlap and interaction, which is then overtaken by the single-particle confinement potential. Increasing V_0 (not shown) has similar effects, as one would expect. We stress that in this structure one has the possibility of changing not only the height of the electrostatic potential well but also the width in such a way that a competition between Coulomb interaction and confinement effects may be explored and modulated.

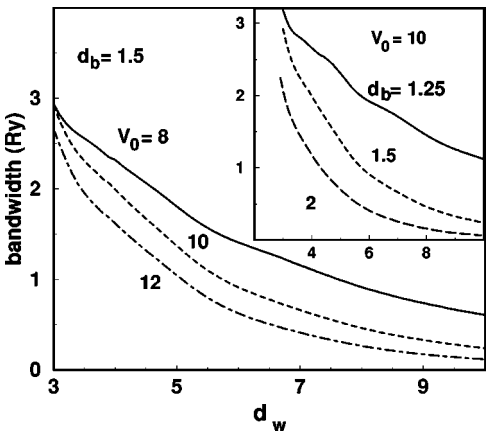

FIG. 2. Bandwidth $E_2^+(q=\pi/d)-E_2^+(q=0)$ for different barrier heights V_0 and $d_b=1.5$. The inset has the same axes and shows bandwidths for different d_b values and $V_0=10$. Larger V_0 and/or d_b and d_w strongly reduce bandwidth.

Figure 1(b) shows typical effective oscillator strength curves for excitonic transitions. We estimate these from the exciton-photon coupling coefficient for direct transitions in the electric dipole approximation,[11]

$$\mathrm{T}_{cv}\propto\mathbf{e}\cdot\mathbf{p}_{cv}\int\Psi(\mathbf{r}_e=\mathbf{r}_0,\mathbf{r}_h=\mathbf{r}_0)d\mathbf{r}_0, \tag{9}$$

where $\mathbf{e}$ is the light polarization vector, and $\mathbf{p}_{cv}$ is the interband optical matrix element of the momentum operator between the conduction and valence bands involved. Notice that $|T_{cv}|^2$ is proportional to the imaginary part of the susceptibility and is then related to the effective absorption coefficient.[11] In agreement with the smaller binding energies, one finds much weaker overlap and strongly reduced absorption, specially for $d_w\gtrsim 6a_0$, as that effectively separates the electron and hole further. Increasing d_b values strongly suppress the oscillator strength, with oscillations vs d_w which are correlated with those in $E_{binding}$, as clearly seen in the three curves here.

Figure 2 shows typical results for the first excited bandwidth $\Delta=E_2^+(q=\pi/d)-E_2^+(q=0)$ as a function of the electrostatic potential dimensions d_w and d_b of the electron well and barrier, respectively. We see that the bandwidths decrease nearly monotonically as d_w increases, keeping V_0 constant, as one would intuitively expect for wider hole barrier d_w. Larger V_0 suppresses tunneling and produces stronger exciton localization to a single period (still in a staggered, type-II, configuration). We should mention, in fact, that the corresponding bandwidth of the lowest exciton band $E_1^+(q)$ for these parameters is quite small ($\lesssim 0.1$ Ry), and varies little over the d_w range studied (not shown). It is clear that as the corresponding single-particle state is quite deep, the periodic potential does not achieve significant exciton delocalization. As shown in the inset, one also finds that as d_b increases, Δ drops rapidly, as the larger electron barrier values also suppress tunneling and induce exciton localization in a single period.

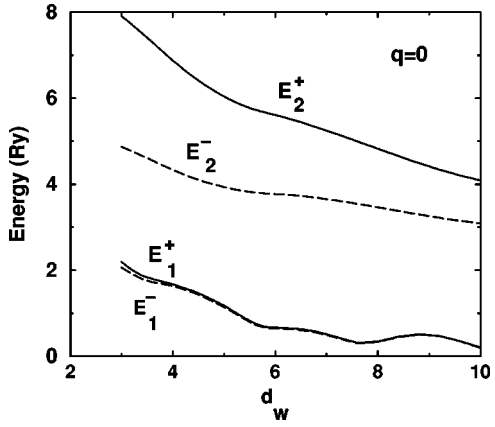

FIG. 3. Exciton energies at Γ point, $E_j^{\pm}(q=0)$, for $V_0=10$ Ry and $d_b=1.25a_0$. Notice near degeneracy of $E_1^{\pm}$, especially for larger d_w.

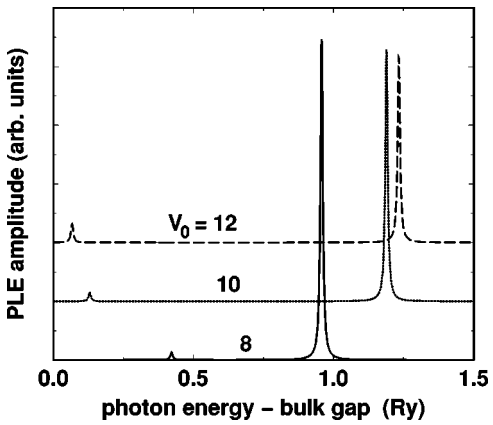

FIG. 4. Ideal PLE yield for folded exciton spectrum. Only E_1^+ (left peaks) and E_2^+ (right peaks) contribute to this range. Strong asymmetry in peak heights reduces for larger V_0. Here $d_b=1.5a_0$ and $d_w=4a_0$, and V_0 values as shown (in Ry). Peak width is set at 0.05 Ry.

Figure 3 shows the Γ-point exciton energy $E_j^{\pm}(q=0)$ as a function of d_w, with $V_0=10$ Ry, and $d_b=1.25a_0$. The dependence shown illustrates the role of symmetry of the intervening single-particle states. For example, $E_j^+-E_j^-$ is a measure of the hole tunneling (and parity), and is correspondingly higher for the ''2'' excited state, than for the lower ''1'' ground state, as the latter lies deeper in the potential well and is more localized. Similarly, the difference between same-parity states, such as $E_2^+-E_1^+$, illustrates the effects of the single-particle confinement due to the d_w well. Although the general features can be understood in terms of a single-particle picture, the oscillations seen in those curves arise from the interplay with the Coulomb interaction, which for specific values of d_w affects the energies more strongly. Similar results are seen for other parameter values, with weaker features for larger d_w or d_b widths.

Finally, and perhaps much more important to experiments, we have calculated the resulting PLE yield of such a system for different parameters. We present in Fig. 4 the exciton density of states weighted by the oscillator strength of each transition/state, $|\mathrm{T}_{cv}|^2$. This quantity describes the intrinsic yield in a PLE experiment, as it gives the relative strengths of the various transitions. As the exciton center-of-mass dispersion ''folds back'' to the Γ point, one would expect additional features to appear in the PLE response. In fact, all the states presented in Fig. 3, $E_j^{\pm}(q=0)$, would be accessible as the first few transitions in the PLE scan, with an amplitude given by their oscillator strength. We should notice, however, that due to symmetry, T_{cv} is *zero* for the odd-parity states E_j^-, and only the even-parity states are accessible. Figure 4 shows this PLE yield for the lowest E_1^+ and E_2^+ states of the exciton. The taller (short) peaks on the right (left) correspond to E_2^+ (E_1^+) as their higher (lower) energy in each well provides for larger (smaller) electron-hole overlap and oscillator strength. Notice that as V_0 increases, the $E_2^+-E_1^+$ separation increases, as one expects for the single-particle states. Notice also that the peak amplitude and asymmetry is reduced substantially, signaling the trend towards the ''infinite-well'' configuration, where the ''exciton'' exists only within one period, no center-of-mass dispersion exists, and all the oscillator strengths vanish. Once again, the V_0 tunability would facilitate the identification of these features in experiments.

In summary, we have studied the effects of electrostatically induced superlattices on the optical properties of the ground and first excited states of Wannier excitons. The resulting band-structure redistributes some of the oscillator strength to the folded center-of-mass exciton modes due to the periodic potential modulation. Oscillations of the exciton binding energies and absorption coefficients are seen as functions of the induced electrostatic potential superlattice parameters in all excitonic states. The excited states show stronger PLE couplings as a result of the stronger overlap of the symmetric wave functions.

In closing, let us mention that we are currently studying how these features are affected in the presence of magnetic field, as it would dramatically affect the carrier confinement along the wires and the resulting optical response.[12]

We thank A. Govorov, W. Hansen, A. D. Hernández de la Luz, J. Kotthaus, and S. Zimmerman for helpful discussions. G.H.C. was partially supported by CONACyT Grant No. 26363-E, Mexico. S.E.U. acknowledges support from the U.S. Department of Energy Grant No. DE-FG02-91ER45334.

[1] See for example, G. Bastard, J. A. Brum, and R. Ferreira, Solid State Phys. **44**, 229 (1991).

[2] C. Peters, W. Hansen, J. P. Kotthaus, and M. Holland, J. Phys. IV **3**, 123 (1993).

[3] A. Schmeller, W. Hansen, J. P. Kotthaus, and G. Trankle, Appl. Phys. Lett. **64**, 330 (1994).

[4] S. Zimmermann, G. Schedelbeck, A. G. Govorov, A. Wixforth, J. P. Kotthaus, M. Bichler, W. Wegscheider, and G. Abstreiter, Appl. Phys. Lett. **73**, 154 (1998).

[5] M. M. Dignam and J. E. Sipe, Phys. Rev. B **43**, 4084 (1991).

[6] M. Matsuura and Y. Shinozuka, Phys. Rev. B **38**, 9830 (1988).
[7] G. W. Bryant, Phys. Rev. B **46**, 1893 (1992); **37**, 8763 (1988).
[8] J. Cen and K. K. Bajaj, Phys. Rev. B **46**, 15 280 (1992).
[9] Although the finger gate used to create the electrostatic modulation has sharp profiles, a realistic potential in the region of the quantum well below is smoother, since the high Fourier components decay faster into the material. For simplicity, however, we approximate the potential by a sequence of square profiles. This should have no qualitative effect in our main conclusions, as we will see below.
[10] G. H. Cocoletzi and S. E. Ulloa, Phys. Rev. B **49**, 7573 (1994).
[11] R. J. Elliot, Phys. Rev. **108**, 1384 (1957).
[12] A. D. Hernández de la Luz, G. H. Cocoletzi, and S. E. Ulloa (unpublished).